ELSEVIER

Chemical Physics 211 (1996) 47–71

Chemical Physics

Solvent reorganization energy of electron transfer in weakly polar solvents

Dmitry V. Matyushov

Department of Chemistry, Colorado State University, Fort Collins, CO 80523, USA

Received 7 March 1996

Abstract

The paper reports a molecular treatment of intramolecular electron transfer (ET) reactions in weakly polar solvents. The theoretical analysis based on the perturbation expansion over solute-solvent interactions focuses on the following issues: (i) the relative contribution of induction, dispersion and dipole–dipole intermolecular forces to the ET activation parameters, (ii) the comparative participation of dipole orientational and molecular translational solvent modes in activating ET, and (iii) the effect of solvent molecularity on temperature variation of ET rates. The theory is tested on the experimentally studied intramolecular charge separation reaction. For the system considered, the dispersion and dipolar components of the energy gap vary oppositely but to a comparable magnitude with solvent polarity. Translational solvent modes were found to be increasingly important for less polar solvents. The difference in activation mechanisms in polar and nonpolar fluids is rooted in different weights of orientational and translational modes in the solvent response. The translational contribution results in a maximum in the Arrhenius coordinates experimentally reported for butyl acetate as the solvent and reproduced by the present theory. The continuum treatment of solvent effects is shown to be incapable of describing this phenomenon.

1. Introduction

The solvent reorganization energy (SRE) of electron transfer (ET) reactions in condensed media, throughout below denoted λ_s, is a fundamental parameter determining the solvent effect on the reaction activation barrier. For classical solvent modes, λ_s characterizes the energetic strength of gaussian medium fluctuations with the spectral width $\Delta^2 = 2k_BT\lambda_s$. In the linear response approximation, λ_s arises also as a summand in the ET absorption energy together with the equilibrium energy gap ΔG^0 (the intramolecular solute modes are neglected),

$$\hbar\omega_{abs} = \Delta G^0 + \lambda_s. \tag{1}$$

This expression is the basis for studying solvent reorganization effects by means of optical spectroscopy methods [1–4].

The most widely used mechanism of ET activation by solvent modes is that of orientational fluctuations of the medium permanent dipoles [5,6]. The key features of this model are (i) orientations of the permanent dipoles is the only *inertial* medium mode and (ii) the high-frequency electronic polarization is adiabatically

PII S0301-0104(96)00198-X

excluded. The physical realization of such a model is a frozen medium (solid or glass) composed of permanent dipoles with no translations. The reorganization energy λ_s is commonly calculated by representing the medium as a dielectric continuum [6]. This, additionally to frozen translations, implies that on the characteristic solute lengths (reactant radii and the donor–acceptor separation) the finite-size dipolar molecules may be replaced by point-sized dipoles. The solvent reorganization energy is then represented as the continuum solvation energy of the ET dipole caused by the electronic transition. Because the continuum treatments are long known to overestimate charge solvation energies, initial molecular-based descriptions of solvent reorganization have been sought in terms of liquid state theories of ion solvation. The Wolynes dynamic extension [7] of the mean-spherical approximation (MSA) for ion-dipolar mixtures [8] was applied to construct molecular-based expressions for λ_s [9–11]. Discarding though the continuum assumption of the point-size dipolar molecules, these treatments are yet confined to the concept of orientational dipole fluctuations owing to the fact that the MSA disregards the positional correlations and thus the translational fluctuations in the liquid. However, for any realistic model of charge relocalization in liquid solvents, the liquid translational degrees of freedom are to be incorporated as well [12–14]. This improvement implies the involvement of the *inertial* solvent mode of molecular translations in addition to orientational modes as in the original concept of ET activation. Translational fluctuations, in turn, bring about new mechanisms of ET activation absent in a frozen medium of the continuum and MSA treatments. These are: (i) activation by induction and dispersion forces [15,16] and (ii) translations of permanent dipoles [17,18]. Whereas the latter mechanism, along with dipolar orientations, is peculiar to polar fluids, the former remains also for nonpolar solvents. The implication of dispersion and induction forces is capable of explaining nonzero SREs experimentally observed in nonpolar fluids [19–27].

Translational solvent modes have been shown to result in an explicit $\propto 1/T$ temperature dependence of the corresponding components of λ_s which may manifest itself in a maximum in the Arrhenius coordinates for small activation barriers [16,28]. Consistent with the mechanism of translational fluctuations, such maxima have been observed experimentally in weakly polar [29] and nonpolar [19,30] solvents, where translational activation is expected to dominate. In view of these experimental findings, an extension of the theory first formulated for nonpolar fluids [15,16] to weakly polar ones seems to be timely. The present work provides therefore a molecular-based description of ET in weakly polar liquids aimed at comparing the theory predictions with experimental ET activation parameters. The two main points of concern in this treatment are the solvent polarity dependence of the SRE and the temperature dependence of ET rates. The molecular treatment employed here allows us to project out the components of λ_s arising from different types of solute-solvent interactions. Along these lines, the differences in mechanisms of ET in strongly and weakly polar liquids can be traced to different weights of orientational and translational modes in thermal activation: the former prevailing in strongly polar and the latter in weakly polar solvents. As we shall see in what follows, translational activation of ET in weakly polar solvents provokes a maximum in the Arrhenius coordinates, in line with experiment.

Several computational treatments of ET energetics employing simulation techniques [31,32], density functional [33] and reaction field [34] approaches and interaction-site models [35,36] have emerged recently in the literature. They are capable of providing a more specific description of solvent effects than the perturbation treatment utilized in this work, but still do not incorporate some physically important features of solute-solvent interactions. First, both solute and solvent [31,35] or only solute [33,36] are treated as nonpolarizable objects. Both properties are however included in the present theory. The role of the solute and solvent polarizabilities is twofold: (i) renormalization of the solute and solvent dipole moments and (ii) activation of electron transitions through induction and dispersion forces which fluctuations are caused by molecular translations. The consideration is thus restricted by the weak donor–acceptor coupling limit [37,38] when the transferred electron is loosely bound compared to the solvent electrons and the electronic time scales of solute and solvent are well separated. Second, differential solvation by dispersion forces in the initial and final states is traditionally neglected. The latter assumption becomes however erroneous for intramolecular transitions in bulky donor–acceptor complexes (DAC) resulting in a substantial variation of the solute polarizability, as it actually happens for the ET system the theory is applied to. Further, the problem of temperature variation of ET rates remains still beyond the

consideration of molecular-based theoretical studies. As a result, the only available way of treating the solvent dependence of ET enthalpies and entropies is through the temperature dependent solvent dielectric constants of linearized continuum theories. However, a continuum description is shown below to be incapable of reproducing the maximum in the Arrhenius coordinates being thus a purely molecular phenomenon.

The remainder of this paper is organized as follows: In Section 2 the general dissection of the SRE to the components due to different solute-solvent interactions is discussed. Section 3 presents the procedure of calculating the effective radius of the DAC, the equilibrium energy gap and the nonpolar part of the SRE. The theory is applied to experiment in Section 4. In Section 5 the paper is finished with a brief summary. Since the theory involves a great number of parameters, they are summarized for convenience in Appendix B.

2. General relations

We consider here ET in a DAC interacting with the surrounding liquid solvent via dipolar (permanent and induced) and dispersion forces. The electronic transition leads to the change in the DAC vacuum electric field $\Delta \boldsymbol{D}(\boldsymbol{r})$ associated with the ET dipole moment Δm. The field variation produces the difference in interaction energies with permanent and induced solvent dipoles. Although induced dipoles follow instantaneously the variation in the solute multipole charge, the induction forces $\propto \Delta m \alpha_s / r^6$ (α_s is the solvent molecular polarizability) are dependent on the solvent center-of-mass coordinates. Translations of the solvent induced dipoles are therefore capable of inducing electron transitions. Another solute property which may vary with electronic transitions is the solute polarizability α_0 [39–41]. The variation $\Delta\alpha_0$ is responsible for the differing solute-solvent dispersion interaction energies in the initial and final states [42–44]. Consequently, if the dipole moment and the polarizability are the only solute molecular properties varying in the course of the electronic transition, three types of solute-solvent interactions, that is, (i) dipole–dipole, (ii) induction and (iii) dispersion forces, are responsible for the ET thermal activation by the solvent inertial modes including dipolar orientational and center-of-mass translational. These activation mechanisms are considered in the present paper as promoting electronic transitions.

In continuum treatments, λ_s can be represented through the solvation free energy of the ET dipole Δm. For a model liquid of molecules bearing permanent dipoles and possessing zero molecular polarizabilities, the SRE of intramolecular ET is also defined through the solvation chemical potential of the dipole Δm [45,46]. For this model, due to different symmetries of translational and orientational fluctuations, the total SRE splits into the dispersion $\lambda_{\rm disp}$ and dipolar $\lambda_{\rm dip}$ components

$$\lambda_s = \lambda_{\rm disp} + \lambda_{\rm dip}.$$

For the more realistic case of a polarizable fluid we have to include the induced molecular dipoles and the description becomes more complicated. In nonpolar fluids, the induction and dispersion components contribute additively to λ_s [16]. Yet for polar-polarizable fluids the permanent and induced dipole components can be coupled. In the absence of a general theoretical treatment of ET in such solvents, we assume here these components to be decoupled and will consider λ_s in the form

$$\lambda_s = \lambda_{\rm disp} + \lambda_{\rm ind} + \lambda_{\rm dip}, \tag{2}$$

where $\lambda_{\rm ind}$ is the SRE due to the induction solute-solvent interactions and $\lambda_{\rm dip}$ refers to the effect of the molecular permanent dipoles.

The dipolar reorganization energy $\lambda_{\rm dip}$ is derived as the first order perturbation over the differential interaction energy $-\int \Delta \boldsymbol{D}(\boldsymbol{r}) \delta \boldsymbol{P}(\boldsymbol{r}) d\boldsymbol{r}$ with the solvent polarization fluctuations $\delta \boldsymbol{P}(\boldsymbol{r})$. In the Fourier space, $\lambda_{\rm dip}$ is

$$\lambda_{\rm dip} = \frac{\beta}{2V} \sum_{\alpha,\beta} \int \frac{d\boldsymbol{k}_1 d\boldsymbol{k}_2}{(2\pi)^6} \Delta D_\alpha(\boldsymbol{k}_1) \Delta D_\beta(\boldsymbol{k}_2) \langle \delta P_\alpha(-\boldsymbol{k}_1) \delta P_\beta(-\boldsymbol{k}_2) \rangle^s, \tag{3}$$

where ΔD_α and ΔP_α are the Cartesian projections of the Fourier components $\Delta \boldsymbol{D}(\boldsymbol{k})$ and $\delta \boldsymbol{P}(\boldsymbol{k})$, respectively; V is the solvent volume and $\beta = 1/k_B T$. Since in deriving Eq. (3) the expansion is performed in terms of only the long-range solute-solvent dipolar coupling, the average $\langle \ldots \rangle^s$ includes the short-range solute-solvent forces determining the spatial solute-solvent correlations. This average involves the three-particle solute-solvent-solvent distribution function $g_{0ss}(012)$ which is generally unknown but can be evaluated using the Kirkwood superposition approximation

$$g_{0ss}(012) = g_{0s}(r_1) g_{0s}(r_2) g_{ss}(12). \tag{4}$$

In Eq. (4), "0" indicates the solute, $1 = \{\boldsymbol{r}_1, \Omega_1\}$ includes the molecular coordinate $\boldsymbol{r}_1$ and orientation Ω_1, $g_{0s}(r)$ and $g_{ss}(12)$ are, respectively, the solute-solvent and solvent-solvent pair distribution functions. With account for Eq. (4) λ_{dip} can be rewritten in the r-space

$$\lambda_{\mathrm{dip}} = \frac{\beta\rho}{2}\left[\int (\boldsymbol{m}\cdot\Delta\boldsymbol{D}(\boldsymbol{r}))^2 g_{0s}(r)\,d\Gamma + \rho\int (\boldsymbol{m}_1\cdot\Delta\boldsymbol{D}(\boldsymbol{r}_1))\, g_{0s}(r_1)\,d\Gamma_1 \int h_{ss}(12)(\boldsymbol{m}_2\cdot\Delta\boldsymbol{D}(\boldsymbol{r}_2))\, g_{0s}(r_2)\,d\Gamma_2\right], \tag{5}$$

where $d\Gamma = d\boldsymbol{r}\,d\Omega/4\pi$, $\boldsymbol{m}$ and ρ are, respectively, the solvent dipole moment and the number density, $h_{ss}(12)$ is the solvent-solvent pair correlation function. The dipolar reorganization energy is thus the sum of two terms: (i) the (first) one-particle summand involving the solute-solvent pair distribution function g_{0s} in the first order and the solvent-solvent correlations in the zero order; (ii) the (second) two-particle term of the second order over g_{0s} and of the first order over h_{ss}. To render this statement more illustrative, we represent λ_{dip} in the diagram form shown by entry (a) of Fig. 1. In our previous work [17,18] the function g_{0s} was further expanded in terms of the Mayer functions

$$g_{0s}(r) = \theta_{0s}(\boldsymbol{r}) + \rho\int h_{ss}^{(0)}(r_{12})\,(\theta_{0s}(\boldsymbol{r}_2) - 1)\,d\boldsymbol{r}_2,$$

where $\theta_{0s}(\boldsymbol{r})$ is a step function equal to zero when $\boldsymbol{r}$ falls in the DAC and equal to unity outside of it; $h_{ss}^{(0)}(r)$ is the spherically symmetrical component of $h_{ss}(12)$. Such an expansion grains the dipolar SRE into two physically differing components

$$\lambda_{\mathrm{dip}} = \lambda_{\mathrm{dip,p}} + \lambda_{\mathrm{dip,d}} \tag{6}$$

of solvent dipoles' reorientation $\lambda_{\mathrm{dip,p}}$ and density $\lambda_{\mathrm{dip,d}}$ reorganization. To the second order in the solvent density, they can be represented by the diagrams shown in the entries (b) and (c) in Fig. 1. In more general terms, the splitting of λ_{dip} into the orientational and density parts can be performed by applying the relation

$$g_{0s}(r) = \theta_{0s}(\boldsymbol{r}) + h_{0s}(r)\theta_{0s}(\boldsymbol{r}).$$

The orientational term $\lambda_{\mathrm{dip,p}}$ in Eq. (6) appears as a result of replacing the coordinate pair distribution function (PDF) by a step function and is affected by only orientational solvent correlations, whereas the second part takes into account the liquid structure factor. Accordingly, the molecular mechanisms responsible for the separation to $\lambda_{\mathrm{dip,p}}$ and $\lambda_{\mathrm{dip,d}}$ are the permanent dipoles reorientations and translations, respectively.

In order to accommodate the variation of the local solvent structure around a solute undergoing an electronic transition, Bader and Berne [47] have recently utilized the state dependent solute radius in the continuum dielectric equations for λ_{dip}. The radius has been defined as the distance to the first maximum of the solute-solvent radial distribution function. Though the underlying ideology involves the density component of the SRE, the procedure seems to be not wholly warranted. The linear response approximation basic for that development utilizes an expansion over the variation of the slowly varying long-range multipole interaction

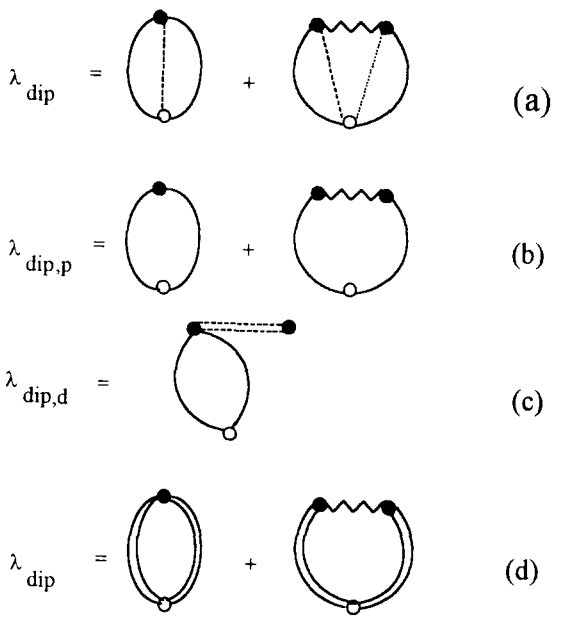

Fig. 1. Diagram representation of the dipolar reorganization energy λ_{dip} (a) and its decomposition into the orientational $\lambda_{dip,p}$ (b) and density $\lambda_{dip,d}$ (c) constituents. (d) shows λ_{dip} according to the surrogate treatment by Perng et al. [36]. The diagrams' parts denote: ——— = $(\boldsymbol{m}\cdot\Delta\boldsymbol{D}(\boldsymbol{r}))$, ∧∧∧ = $h_{ss}(12)$, :::::: = $h_{ss}^{(0)}$, ═══ = $(\boldsymbol{m}\cdot\Delta\boldsymbol{D}_{\Sigma}(\boldsymbol{r}))$, – – –– = $g_{0s}(r)$, ○ = solute, • = ρ × solvent, and the integration is performed over the solvent coordinates and orientations.

(e.g., $(\boldsymbol{m}\cdot\Delta\boldsymbol{D}(\boldsymbol{r}))$) imposing a weak perturbation on the solvent. The change in the solute size produces a huge, at contact solute-solvent separations, variation of the repulsion potential. For this part a special procedure should be employed. Solely the renormalization of the solute radius when applied to evaluating the transition and reorganization energies leaves obscure the choice of the reference system for the perturbation expansion.

Perng et al. [36] have recently proposed a molecular formulation of the solvent reorganization problem in terms of the interaction-site model for both the solute and the solvent. Their theory operates with the SRE in the form analogous to $\lambda_{dip,p}$ but, to include the local structure around the solute, the factual solute field $\Delta\boldsymbol{D}(\boldsymbol{r})$ is replaced by a surrogate expression $\Delta\boldsymbol{D}_{\Sigma}(\boldsymbol{r})$ proportional to the solute-solvent site-site direct correlation function. The surrogate solute-solvent interaction involves thus the spatial solute-solvent correlations. The treatment is the extension of the approach fist proposed to describe the solvation dynamics [48]. The SRE in the theory of Perng et al. [36] can be represented by the diagram (d) in Fig. 1. As is seen from comparison of the diagrams (a) and (d) in Fig. 1, the one-particle first summand in the surrogate treatment [36] is effectively quadratic in g_{0s}, in contrast to the exact expansion (5). This calculation scheme is therefore a possible source of overestimating λ_{dip} which is higher approximately to the value of

$$(\beta\rho/2)\int(\boldsymbol{m}\cdot\Delta\boldsymbol{D}(\boldsymbol{r}))^2\,h_{0s}(r)\,d\Gamma.$$

The orientational reorganization energy

$$\lambda_{dip,p}=\frac{\beta}{2V}\sum_{\alpha}\int\frac{d\boldsymbol{k}}{(2\pi)^3}|\Delta D'_{\alpha}(\boldsymbol{k})|^2\langle|\delta P_{\alpha}(-\boldsymbol{k})|^2\rangle, \tag{7}$$

is the usual for ET and dipolar relaxation theories SRE containing only the homogeneous correlation function of the liquid polarization fluctuations; $\Delta\boldsymbol{D}'(\boldsymbol{k})$ is the Fourier transform of $\Delta\boldsymbol{D}(\boldsymbol{r})\theta_{0s}(\boldsymbol{r})$. Eq. (7) can be written more conveniently in terms of the longitudinal (L) and transverse (T) projections

$$\lambda_{\mathrm{dip,p}} = \frac{\beta\rho m^2}{6}\int \frac{d\boldsymbol{k}}{(2\pi)^3}\left[m^+(k)|\Delta D'_L(k)|^2 + 2m^-(k)|\Delta D'_T(k)|^2\right], \tag{8}$$

relating the solvent response to the longitudinal $m^+(k)$ and transverse $m^-(k)$ structure factors. The functions $m^{\pm}(k)$ are determined by the equilibrium Fourier-space correlation functions of the longitudinal $\delta P_L(\boldsymbol{k})$ and transverse $\delta P_T(\boldsymbol{k})$ solvent polarization fluctuations

$$\langle \delta P_L(-\boldsymbol{k})\delta P_L(\boldsymbol{k})\rangle = \frac{Nm^2}{3}m^+(k), \tag{9}$$

$$\langle \delta P_T(-\boldsymbol{k})\delta P_T(\boldsymbol{k})\rangle = \frac{Nm^2}{3}m^-(k). \tag{10}$$

where N is the number of liquid molecules. Eq. (8) is the general relation for the orientational SRE. A particular form of $\lambda_{\mathrm{dip,p}}$ depends on the model adopted for the DAC charge distribution and for the structure factors $m^{\pm}(k)$. In the continuum solvent description, the k-dependence in $m^{\pm}(k)$ is disregarded and the macroscopic values $m^{\pm}(k) = m^{\pm}(0)$ are assumed in Eq. (8). If the high-frequency electronic polarization is adiabatically excluded in the continuum approximation [18], $\Delta\boldsymbol{D}(r)$ in Eq. (8) attains the "screening" factor $\Delta\boldsymbol{D}(r) \to q\Delta\boldsymbol{D}(r)$, $q = (\epsilon_\infty + 2)/3\epsilon_\infty$ and [49]

$$m^+(0) = \frac{1}{3y_0q^2}\left(\frac{1}{\epsilon_\infty} - \frac{1}{\epsilon_s}\right), \qquad m^-(0) = \frac{1}{3y_0q^2\epsilon_\infty^2}(\epsilon_s - \epsilon_\infty). \tag{11}$$

where $y_0 = (4\pi/9)\beta\rho m^2$; ϵ_∞ and ϵ_s are the high-frequency and static solvent dielectric constants, respectively. The continuum SRE attains therefore the form

$$\lambda^{(c)}_{\mathrm{dip,p}} = \frac{c_0}{2}\int_0^\infty \frac{k^2dk}{(2\pi)^3}\left[|\Delta D'_L(k)|^2 + \frac{2\epsilon_s}{\epsilon_\infty}|\Delta D'_T(k)|^2\right], \tag{12}$$

where $c_0 = 1/\epsilon_\infty - 1/\epsilon_s$ is the Pekar factor. For outer-sphere ET, $\Delta\boldsymbol{D}(\boldsymbol{r})$ is commonly represented by that of a pair of infinitely separated oppositely-charged spherical sites [6] and we have

$$\Delta D'_L(k) = -(4\pi ie/k)\left[j_0(kR_\mathrm{d}) - j_0(kR_\mathrm{a})\exp(-i\boldsymbol{kR})\right], \tag{13}$$

$$\Delta D'_T(k) = 0, \tag{14}$$

where $j_n(x)$ is the spherical Bessel function of order n, R_d and R_a are the radii of the donor and acceptor moieties, and R is the donor–acceptor separation. Substituting Eqs. (13) and (14) into Eq. (12) we get the well-known [6] relation

$$\lambda^{(c)}_{\mathrm{dip,p}} = \frac{c_0e^2}{2}\left(\frac{1}{R_\mathrm{a}} + \frac{1}{R_\mathrm{d}} - \frac{2}{R}\right), \tag{15}$$

where e is the electron charge. For intramolecular ET, the DAC can often be represented by a sphere of the effective radius R_0 with $\Delta\boldsymbol{D}(\boldsymbol{r})$ modeled by the point dipole field. In this case,

$$\Delta D'_L(k) = -8\pi\Delta m j_1(kR_0)/kR_0, \qquad \Delta D'_T(k) = 4\pi\Delta m j_1(kR_0)/kR_0$$

and $\lambda_{\mathrm{dip,p}}$ takes the form

$$\lambda^{(c)}_{\mathrm{dip,p}} = \frac{c_0(\epsilon_s + 2\epsilon_\infty)}{\epsilon_\infty}\frac{\Delta m^2}{3R_0^3}. \tag{16}$$

Since the transverse structure factor $m^-(0)$ diverges with increasing solvent polarity $\epsilon_s \to \infty$, the intramolecular SRE bears the same feature. This is the case for any model of $\Delta\boldsymbol{D}(\boldsymbol{k})$ containing a transverse component:

the transverse part of the solvent response becomes increasingly important with increasing solvent polarity. The solute field $\Delta \boldsymbol{D}(\boldsymbol{k})$ in the form of Eqs. (13) and (14) is actually very unrealistic corresponding to the infinitely separated donor and acceptor sites. For any close to contact donor–acceptor configuration the field $\Delta \boldsymbol{D}(\boldsymbol{k})$ attains inevitably a transverse component resulting in a diverging at $\epsilon_s \to \infty$ part of the SRE. This problem of general character has gained up till now surprisingly little attention in the literature. [The only work addressing the problem we aware of is that by Chandra and Bagchi [50] where the influence of the transverse response on the characteristic time of dipolar relaxation has been considered]. Note also that the transverse response does not appear in the relations for the reorganization energy when interaction site models [36,48] are applied. This feature seems to be buried in the nature of the interaction site method operating in terms of the angular averaged site-site distribution functions.

Since we use here the solute description as a spherical core with a centered dipole, to go around the problem of the expansion divergence, we apply the representation of the dipolar reorganization energy through the chemical potential of dipole solvation by the inertial solvent modes [51]. To this end, we employ the Lippert [52] procedure of determining the absorption optical transition energy $\hbar\omega_{\rm abs}$ as follows.

Instantaneous excitation of the solute produces adiabatic solvation of the excited state by the inertialess solvent and solute modes and creates the state of strain for the inertial modes. Dispersion and induction solute-solvent forces caused by virtual intramolecular electronic excitations belong to inertialess modes, whereas molecular orientations and coordinates are inertial modes remaining equilibrated to the ground state charge distribution immediately after excitation. If intramolecular solute excitation results in the variation of the solute dipole moment, $m_{\rm g} \to m_{\rm e}$, and polarizability, $\alpha_{\rm g} \to \alpha_{\rm e}$ ($\alpha_{\rm g} = \alpha_0$), the absorption energy shifts from the vacuum value ΔI to the energy

$$\hbar\omega_{\rm abs} = \Delta I + \Delta G_{\rm disp} - \int_{m_{\rm g}}^{m_{\rm e}} R^{\infty}(m')\,dm' - R_{\rm g}^{\rm in}(m_{\rm e} - m_{\rm g}), \tag{17}$$

where R^{∞} and $R^{\rm in}$ are the reaction fields of high-frequency inductions and inertial dipole orientations, respectively; the subscripts "g" and "e" denote the ground and excited states, respectively. In Eq. (17), $\Delta G_{\rm disp} \propto \Delta\alpha$, $\Delta\alpha = \alpha_{\rm e} - \alpha_{\rm g}$ is the variation of the free energy of the dispersive solute-solvent interaction. (Notice that Eq. (17) includes only the first nonvanishing terms in the expansion of the solvent response over $\Delta\alpha$. The second order perturbation terms are enclosed in the nonpolar reorganization energy discussed below in Section 3.3.)

The reaction field is defined as the derivative of the chemical potential of dipole solvation $\mu_p(m_0)$ over the solute dipole moment m_0, $R = -\partial\mu_p(m_0)/\partial m_0$. For the inertial reaction field $R^{\rm in}$, we should take the chemical potential due to the permanent dipoles reorientation which is given by the difference of the total chemical potential μ_p and the potential μ_p^{∞} due to only induced dipoles

$$R_{\rm g}^{\rm in} = -\frac{\partial}{\partial m_0}\left[\mu_p(m_0) - \mu_p^{\infty}(m_0)\right]\Big|_{m_{\rm g}}.$$

In the similar way, the inertialess reaction field is related only to the high-frequency part μ_p^{∞} of the chemical potential

$$R^{\infty}(m_0) = -\frac{\partial\mu_p^{\infty}(m_0)}{\partial m_0}.$$

In the linear response approximation employed here the chemical potential of dipole solvation is given by only the first term of the perturbation expansion over the solute dipole moment $\mu_p(m_0) = m_0'^2\Psi_p$, $\mu_p^{\infty}(m_0) = m_0^{\infty 2}\Psi_p^{\infty}$, where Ψ_p and Ψ_p^{∞} are the expansion coefficients often termed the response functions. In this expansion, m_0' and m_0^{∞} denote the solute dipole moments enhanced relative to the vacuum value m_0 due to

a nonzero solute polarizability interacting with, respectively, total R and high-frequency R^{∞} solvent reaction fields

$$m_0' = m_0 \Big/ \left(1 - \frac{\alpha_0}{m_0'} R\right), \qquad m_0^{\infty} = m_0 \Big/ \left(1 - \frac{\alpha_0}{m_0^{\infty}} R^{\infty}\right).$$

Under the assumption of the linear response we get

$$\hbar\omega_{\mathrm{abs}} = \Delta I + \Delta G_{\mathrm{disp}} - 2m_{\mathrm{g}}'(m_{\mathrm{e}}' - m_{\mathrm{g}}')\Psi_p - \left(m_{\mathrm{e}}^{\infty} - m_{\mathrm{g}}^{\infty}\right)^2 \Psi_p^{\infty}. \tag{18}$$

Analogously, for the fluorescence energy $\hbar\omega_{\mathrm{fl}}$ we get

$$\hbar\omega_{\mathrm{fl}} = \Delta I + \Delta G_{\mathrm{disp}} - 2m_{\mathrm{e}}'(m_{\mathrm{e}}' - m_{\mathrm{g}}')\Psi_p + \left(m_{\mathrm{e}}^{\infty} - m_{\mathrm{g}}^{\infty}\right)^2 \Psi_p^{\infty}.$$

The dipole component of the SRE is determined as the one-half of the Stokes shift $\hbar\Delta\omega_{\mathrm{st}} = \hbar(\omega_{\mathrm{abs}} - \omega_{\mathrm{fl}})$ as follows

$$\lambda_{\mathrm{dip}} = \left(m_{\mathrm{e}}' - m_{\mathrm{g}}'\right)^2 \Psi_p - (m_{\mathrm{e}}^{\infty} - m_{\mathrm{g}}^{\infty})^2 \Psi_p^{\infty}. \tag{19}$$

For explicit calculations, the dipolar response functions Ψ_p and Ψ_p^{∞} are needed. Two known analytical approximations, the Onsager [53] and the MSA [54–56] theories, yield upward [57,58] and downward [59] estimates of Ψ_p. On the other hand, the recently proposed Padé form of the dipolar response falls between the two approximations and has been shown to be capable of reproducing the polarity dependence of experimental dipole solvation energies [60]. In that framework, the chemical potential of solvation μ_p of a spherical solute of the radius R_0 with centered dipole m_0 is given as an extension of the Wertheim theory of polar-polarizable fluids [61] to the solvation case and can be written as

$$\mu_p^{\mathrm{P}} = -\frac{1}{\sigma^3}\left[\tilde{m}^2 P(y,\rho^*,r_0) - \frac{3\alpha_0}{\beta} P(y_{\infty},\rho^*,r_0)\right] + u_{0p}, \tag{20}$$

$$u_{0p} = \left(2m_0'^2\alpha_0/\sigma^6\right) P(y,\rho^*,r_0), \qquad \tilde{m}^2 = m_0'^2 + 3\alpha_0/\beta,$$

where the vacuum solute dipole moment is renormalized in the liquid due to a nonzero solute polarizability to

$$m_0' = m_0\left[1 - \frac{2\alpha_0}{\sigma^3} P(y,\rho^*,r_0)\right]^{-1}.$$

In Eq. (20), $P_1 = P(y,\rho^*,r_0)$ and $P_2 = P(y_{\infty},\rho^*,r_0)$ are the Padé forms of the solvent response on the solute dipole moment which depends on the solvent dielectric parameters

$$y = (4\pi/9)\beta\rho m'^2 + (4\pi/3)\rho\alpha_s, \qquad y_{\infty} = (4\pi/3)\rho\alpha_s, \tag{21}$$

the reduced solvent density $\rho^* = \rho\sigma^3$, and the reduced distance of the closest approach of the solvent molecules to the solute $r_0 = 0.5 + R_0/\sigma$, σ is the solvent hard-sphere (HS) diameter. The explicit analytical form of $P(y,\rho^*,r_0)$ is given in Appendix A. In the definition of y above, m' is the dipole moment of a liquid molecule renormalized due to the solvent molecular polarization induced by the field of the surrounding molecules. The effective solvent dipole and consequently the dipolar parameter y are accurately determined by the self-consistency condition of Wertheim theory [61]. Yet an approximate estimate of y can be gained from the combined application of the Kirkwood equation

$$\frac{(\epsilon_s - 1)(2\epsilon_s + 1)}{9\epsilon_s} = g_{\mathrm{K}} y \tag{22}$$

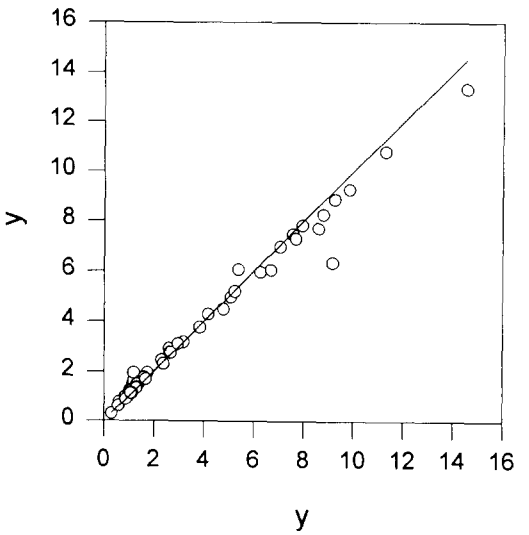

Fig. 2. Plot of dipolar parameters y as defined by Eq. (21) calculated according to Eqs. (22) and (23) vs. those from Wertheim theory [61] for 52 polar liquids (○) from Ref. [62]. The solid line drawn as the guide for the eye represents the equality between the two sets of values.

and the Frölich definition of the Kirkwood g_K factor

$$\frac{(\epsilon_s - \epsilon_\infty)(2\epsilon_s + \epsilon_\infty)}{y_0 \epsilon_s (\epsilon_\infty + 2)^2} = g_K, \tag{23}$$

In Fig. 2, y values obtained from Wertheim theory are compared to those from Eqs. (22) and (23) for 52 polar fluids of Ref. [62].

From Eqs. (19) and (20) we get immediately

$$\lambda_{dip} = (\Delta m/\sigma^3)\left[(m'_e - m'_g)P_1 - (m_e^\infty - m_g^\infty)P_2\right]. \tag{24}$$

Analogously, for the dipolar component of the equilibrium energy gap, from Eqs. (1) and (18) we have

$$\Delta G_{dip} = -\frac{\Delta m}{\sigma^3}(m'_e + m'_g)P_1 - (m_e^{\infty 2} - m_g^{\infty 2})\frac{2\alpha_0}{\sigma^6}P_2^2. \tag{25}$$

The vacuum solute dipole moment difference Δm in Eqs. (24) and (25) arises due to the energy u_{0p} of solute polarization in Eq. (20). This positive contribution to the chemical potential of solvation is the work invested in polarizing the solute dipole moment from the vacuum to the liquid state value. As previously pointed out by Luzhkov and Warshel [63], it can amount to about one half the energy gained from the stabilization of the solute dipole moment by the solvent permanent dipoles. Because of this term the solute polarizability renormalizes the squared transition dipole Δm^2 at $\alpha_0 = 0$ to the product $\Delta m \Delta m'$ in Eq. (24) and not to $\Delta m'^2$ as could *ad hoc* be expected. We shall make use of relations (24) and (25) below in calculating the polarity and temperature dependencies of the activation parameters of intramolecular ET. It is pertinent to note that λ_{dip} in the form of Eq. (24) contains both the orientational $\lambda_{dip,p}$ and the density $\lambda_{dip,d}$ contributions. The former can be extracted in the zero density limit of the Padé forms P_1 and P_2 (see below).

3. Calculation procedure

3.1. Solute effective diameter

The theoretical scheme outlined above has been developed for a spherical solute. Most of experimentally used DACs are however nonspherical objects commonly elongated along the donor–acceptor bond. The application of molecular theories to these systems is complicated by the necessity of knowing the radial PDF of the solvent around a nonspherical solute. The problem can be solved directly in terms of site-site PDFs [35,36,51] or by applying the density expansion of the solute-solvent PDF [17]. The latter way introduces approximations that can presumably lead to an underestimation of the solvent structure effects. An alternative approach would be to determine an effective radius of a spherical solute for which well developed methods of liquid state theories may be applied. The guiding principle of this definition is the observation that the nonpolar solvent response, probed by equilibrium solvation [64] or optical spectral shifts [16,43,65], is primarily affected by the structure of the solute first coordination sphere or, for HS objects, by the contact value of the radial PDF. Therefore, an effective sphere representing the DAC should have, in average, the same contact value of the PDF as the reactants. The contact value of the PDF is reflected by the cavity formation energy $W(\lambda)$ in a fluid. In scaled particle theory (SPT) [66], $W(\lambda)$ is connected to the contact value of the PDF $g(\lambda+0)$ by the relation

$$W(\lambda) = 4\pi\rho k_B T \int_0^{\lambda} g(\lambda'+0)\lambda'^2 d\lambda',$$

where λ is a cavity radius. Thus, the effective radius can be found by equating the cavity formation energy of a nonspheric donor–acceptor complex with that of an effective sphere. There is certainly some ambiguity in the choice of the DAC geometry. Starting from the work of Cannon [67], it is a long tradition to picture the DAC as an ellipsoid in the dielectric continuum of the solvent [3,68]. This representation is probably not always appropriate, since the donor and acceptor sites are commonly the most bulky groups in the DAC. An alternative could be searched in terms of a pair of fused hard spheres of the radii $R_1 = R_a + \sigma/2$ and $R_2 = R_d + \sigma/2$ [4]. For the donor and acceptor of equal radii connected by a bulky bridge moiety, the DAC can be viewed as a spherocylinder. This latter configuration seems to be most suitable for the DAC complex considered in Section 4 below. Therefore we discuss this particular case in more detail.

Let us consider a spherocylinder formed by two spheres of the radius $R_d = R_a$ with the centers separated by the distance R. The free energy of inserting the spherocylinder in a liquid composed HSs of diameter σ is as follows [69]

$$\beta\Delta G_{cyl} = -\ln(1-\eta) + \frac{6\eta}{1-\eta}\left[\tilde{a} + \tilde{l}/4 + \tilde{a}(\tilde{l}+2\tilde{a}) + \tilde{a}^2(\tilde{l}+4\tilde{a}/3)\right] + \frac{18\eta}{(1-\eta)^2}\left[(\tilde{a}+\tilde{l}/4)^2 + \tilde{a}^2(\tilde{l}+4\tilde{a}/3)\right] + 18\eta^3\tilde{a}^2\frac{\tilde{l}+4\tilde{a}/3}{(1-\eta)^3}, \quad (26)$$

where $\tilde{l} = R/\sigma$, $\tilde{a} = R_d/\sigma$ and $\eta = (\pi/6)\rho\sigma^3$ is the solvent packing fraction. To get the radius R_0 of the effective sphere representing the solute, the above energy ΔG_{cyl} is to be equated to the free energy invested in forming the spherical cavity determined here by the Boublik–Mansoori–Carnahan–Starling–Leland (BMCSL) relation [70,71]

$$\beta\Delta G_{sph} = 2\frac{\eta d^3}{(1-\eta)^3} + 3\frac{\eta d^2}{(1-\eta)^2} + 3\frac{\eta d(-d^2+d+1)}{(1-\eta)} + (-2d^3+3d^2-1)\ln(1-\eta), \quad (27)$$

where $d = 2R_0/\sigma$. The dependence of the effective radius R_0 so obtained on the reactant size is plotted in Fig. 3 for different models (including the choice of the largest possible radius $R_0 = R_d + R/2$) and DAC geometries.

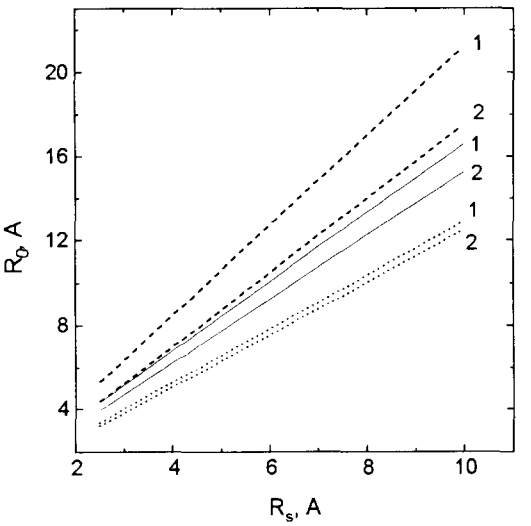

Fig. 3. Radius of the effective sphere representing the DAC R_0 vs. the donor/acceptor size $R_d = R_a$ for different separations of the donor and acceptor sites $R = 2.25R_d$ (1) and $R = 1.5R_d$ (2). The DAC is represented by a pair of fused spheres (dotted lines), as a spherocylinder (solid lines), and by a sphere of the radius $R_0 = R/2 + R_d$ (dashed lines).

Due to the volume between the two spheres cut out by the spherocylinder, the radius R_0 for this geometry is generally larger than that for a pair of fused hard spheres.

The procedure of calculating the effective solute radius through cavity formation energies permits one to get R_0 at a particular temperature, but becomes inadequate for calculating the temperature variation of R_0. This is evident from the general determination of a HS potential as that approximating a real, decreasing with distance, soft repulsive interaction. Under such a definition, R_0 is always decreasing with T: $dR_0/dT < 0$. The definition via the cavity formation energy, on the other hand, does not involve soft repulsions and focuses only on the volume restrictions to the solvent molecules produced by the solute. The result is the unphysical inequality $dR_0/dT > 0$. In view of this deficiency of our procedure, we will put $dR_0/dT = 0$ in the temperature dependence calculations below.

3.2. Free energy gap

The equilibrium energy gap ΔG^0 between the final and initial states is composed of the vacuum energy gap ΔI and the solvent-induced shift due to dipolar ΔG_{dip} and dispersion ΔG_{disp} solvation

$$\Delta G^0 = \Delta I + \Delta G_{dip} + \Delta G_{disp}, \tag{28}$$

where the dipolar component is determined by Eq. (25). The dispersion contribution results from the solute-solvent dispersion forces which are modeled here by the central Lennard-Jones (LJ) solute-solvent potential. This can be written in the London form as following

$$u_{LJ}^{(0s)} = \frac{\alpha_0}{\alpha_s}\frac{8I_0}{I_0 + I_s}\left(\frac{\sigma_{LJ}^{(s)}}{\sigma_{LJ}^{(0s)}}\right)^6 \epsilon_{LJ}^{(s)} u^{(0s)}(r), \qquad u^{(0s)}(r) = \left(\frac{\sigma_{LJ}^{(0s)}}{r}\right)^{12} - \left(\frac{\sigma_{LJ}^{(0s)}}{r}\right)^6,$$

where α_0, α_s and I_0, I_s are polarizabilities and characteristic excitation energies of the solute and the solvent, respectively. The lengths $\sigma_{LJ}^{(0s)}$ and $\sigma_{LJ}^{(s)}$ are, correspondingly, the solute-solvent and solvent LJ diameters, $\epsilon_{LJ}^{(s)}$ is the solvent LJ energy. The variation of the solute polarizability by electronic transition alters the dispersion

solute-solvent forces producing thus the dispersion component of the energy gap. In the Barker–Henderson separation of the LJ potential into the attraction and repulsion parts [72], $\Delta G_{\rm disp}$ can be written in the form

$$\Delta G_{\rm disp} = \Delta\gamma\mu^{(1)}_{\rm disp}, \tag{29}$$

where

$$\mu^{(1)}_{\rm disp} = 96\eta\epsilon^{(s)}_{\rm LJ}\left(\frac{\sigma^{(s)}_{\rm LJ}}{\sigma^{(0s)}_{\rm LJ}}\right)^6 \int_0^\infty u_1^{(0s)}(r)g^{(0)}_{0s}(r)r^2dr, \tag{30}$$

$$\Delta\gamma = \frac{\Delta\alpha_0}{\alpha_s}\frac{2I_0}{I_0+I_s}, \qquad u_1^{(0s)} = u^{(0s)}\theta(r-\sigma^{(0s)}_{\rm LJ}), \tag{31}$$

$g^{(0)}_{0s}$ is the solute-solvent HS PDF and $\theta(x)$ is a step function.

In order to obtain the solvent induced variation of the energy gap, we need to specify the solute parameters in the initial and final states. The initial and final dipole moments can be evaluated at least approximately from the charge centers separation in the DAC. On the other hand, the polarizability of the DAC is generally unknown in the initial as well as in the final states. For charge separation reactions considered below in Section 4, the polarizability of the initial neutral state can be estimated from empirical additivity rules [73] which are however inapplicable to a charge-separated state. Yet the *change* in the solute polarizability, or, more exactly, in the dispersion interaction constant $\Delta\gamma$ of Eq. (31), can be obtained from the solvent dependence of the equilibrium free energy gap. Actually, the $\Delta\alpha_0$ value and the vacuum energy gap ΔI are given, according to Eq. (28), by slope and intercept, respectively, of the plot of $\Delta G^0 - \Delta G_{\rm dip}$ drawn against the parameter

$$\delta = \frac{2I_0}{I_0+I_s}\frac{96\eta\epsilon^{(s)}_{\rm LJ}}{\alpha_s}\left(\frac{\sigma^{(s)}_{\rm LJ}}{\sigma^{(0s)}_{\rm LJ}}\right)^6 \int_0^\infty u_1^{(0s)}(r)g^{(0)}_{0s}(r)r^2dr. \tag{32}$$

The solute polarizability change obtained in this way is, however, based on the specific London form of the solute-solvent dispersion interaction. In this sense, the value $\Delta\alpha_0$ should be regarded as an effective parameter not exactly equal to the variation of the solute polarizability. Corresponding calculations for the real DAC are presented in Section 4. This procedure yields the parameter $\Delta\gamma$ in Eq. (31), otherwise unavailable, which is crucially important for evaluating the dispersion contributions to the free energy gap and the SRE hereafter considered.

3.3. Reorganization of nonpolar component

The reorganization energy due to dispersion forces appears as the second order perturbation term over the solute-solvent dispersion potential [16] $u_1^{(0s)}(r)$

$$\lambda_{\rm disp} = 8\beta\rho\left(\Delta\gamma\epsilon^{(0s)}_{\rm LJ}\right)^2\left(\sigma^{(s)}_{\rm LJ}/\sigma^{(0s)}_{\rm LJ}\right)^{12}\left[\int u_1^{(0s)}(r)^2 g^{(0)}_{0s}(r)d\boldsymbol{r} + \rho\int u_1^{(0s)}(r_1)g^{(0)}_{0s}(r_1)d\boldsymbol{r}_1\int h^{(0)}_{ss}(r_{12})u_1^{(0s)}(r_2)g^{(0)}_{0s}(r_2)d\boldsymbol{r}_2\right], \tag{33}$$

where $h^{(0)}_{ss}$ is its spherically symmetrical component of the correlation function of the neat liquid. In the "stationary-phase" approximation [16], we get

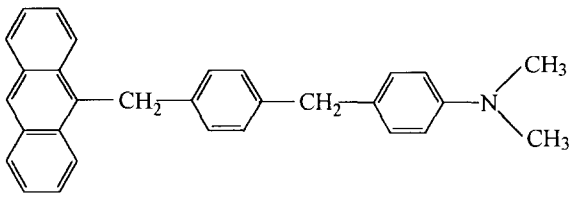

Fig. 4. Structure of the A1D donor–acceptor complex used for the theory–experiment comparison.

$$\lambda_{\rm disp} = 192\beta\eta\left(\Delta\gamma\epsilon_{\rm LJ}^{(0s)}\right)^2\left(\frac{\sigma_{\rm LJ}^{(s)}}{\sigma_{\rm LJ}^{(0s)}}\right)^{12}\left[\int_0^\infty u_1^{(0s)}(r)^2 g_{0s}^{(0)}(r)r^2dr\right.$$
$$\left.-(1-m_{ss}(0))\int_0^\infty u_1^{(0s)}(r)u_1^{(0s)}(r+\varphi)g_{0s}^{(0)}(r)g_{0s}^{(0)}(r+\varphi)r(r+\varphi)dr\right], \tag{34}$$

where φ is the packing density dependent "phase shift" $\varphi = \varphi(\eta)$ [16]. $m_{ss}(0)$ in Eq. (34) is the $k = 0$ value of the structure factor of the neat liquid. It is connected to the liquid compressibility β_T by the relation $m_{ss}(0) \equiv k_{\rm B}T\rho\beta_T$ and for the Percus–Yevick HS liquid is given by $m_{ss}(0) = (1-\eta)^4/(1+2\eta)^2$. The energy $\lambda_{\rm disp}$ in Eq. (34) is proportional to the squared value of $\Delta\gamma$ which becomes therefore a crucial parameter for determining the dispersion contribution to solvent reorganization.

The induction component of the SRE appears as a term of the fourth order in the solute transition dipole, since already the induction solute solvent interaction appears as the second order perturbation over the solute field. In the perturbation expansion over the solute-solvent interaction potential we have [17] for the reorganization energy due to the solute-solvent inductions

$$\lambda_{\rm ind} = \frac{\beta}{\eta}\left(\frac{3\Delta m'^2 y_\infty}{20\sigma^3}\right)^2\left[4\left(2m_\infty^+(0)+m_\infty^-(0)\right)-9\right]\int_{r_0}^\infty \frac{dr}{r^{10}}g_{0s}^{(0)}(r). \tag{35}$$

In Eq. (35), $m_\infty^+(0)$ and $m_\infty^-(0)$ are the $k = 0$ values of the longitudinal and transversal high-frequency dipolar structure factors of the neat liquid. They are related to correlation functions of polarization fluctuations due to the liquid induced dipoles similar to Eqs. (9) and (10) and can be connected to the dielectric parameter y_∞ and the high-frequency dielectric constant ϵ_∞ by the expressions

$$m_\infty^+(0) = \frac{1}{3y_\infty}\left(1-\frac{1}{\epsilon_\infty}\right), \qquad m_\infty^-(0) = \frac{1}{3y_\infty}(\epsilon_\infty - 1).$$

4. Results and discussion

The procedure outlined in the previous sections is applied now to intramolecular charge separation in the A1D DAC extensively studied previously [29,74–76]. Our choice was guided by the fact that the curved Arrhenius dependencies of ET rates analogous to those predicted by theory [15,16] have been observed experimentally for this particular system [29] in weakly polar butyl acetate, diethyl ether and diisopropyl ether solvents. Therefore, the goal of this section is to reproduce the observed maximum and to provide insight on the solvent variation of the SRE components caused by different types of intermolecular interactions.

The A1D complex used for the theory–experiment comparison is the bridged compound of the anthracene acceptor moiety and the donor dimethylaniline residue (Fig. 4). Optical excitation of the anthracene site with the excitation energy $E_{\rm ex} = h\nu_{\rm ex}$ produces the state with the energy much higher than that of the donor (Fig. 5).

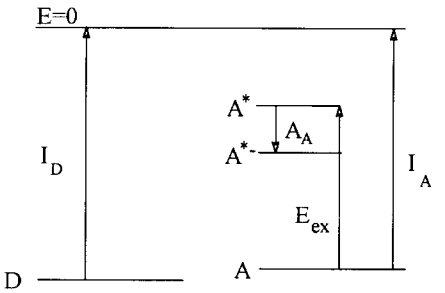

Fig. 5. Positioning of the energy levels in the A1D donor–acceptor complex. In the diagram: I_A and I_D are the acceptor and donor ionization potentials, E_{ex} is the optical excitation energy and A_A is the electron affinity of the excited acceptor. D and A denote the donor and acceptor, respectively.

Due to the high positive energy gap ΔI ET cannot proceed in the gas phase, but becomes possible in polar solvents solvating the charge separated state and thus lowering the equilibrium energy gap from ΔI to ΔG^0. As is schematically shown in Fig. 5, the gas phase energy gap can be estimated from ionization potentials $I_{D,A}$ and electron affinities $A_{A,D}$ of the donor and acceptor moieties according to the following relation

$$\Delta I = I_D - I_A + h\nu_{ex} - A_A - \frac{e^2}{\epsilon_{eff} R}, \tag{36}$$

where $h\nu_{ex} = 3.43$ eV is the vacuum excitation energy of anthracene [77]. The last term in Eq. (36) corresponds to the Coulombic attraction between the positive donor charge and the electron in the acceptor state screened by the effective dielectric constant ϵ_{eff} of the DAC. For dimethylaniline and anthracene moieties $I_D = 7.51$ eV and $I_A = 7.41$ [78]. The electron affinity of the excited anthracene is unknown, but for the ground state a value of 0.6 eV has been reported [79]. Thus the vacuum energy gap should range from 1.3 eV for $\epsilon_{eff} = 1$ to 2.1 eV for $\epsilon_{eff} = 2$.

The DAC A1D can be viewed as composed of the donor and acceptor moieties of radii $R_a = R_d = 4$ Å centers of which are separated by the distance $R = 9$ Å. Because of the bulky bridge group, the complex can be considered as a spherocylinder. The slightly solvent dependent radius of the effective sphere is evaluated from Eqs. (26) and (27) to be 6.7–6.9 Å. The ground state polarizability found from empirical additivity rules [73] amounts to 55 Å^3. However, the initial state preceding ET is achieved experimentally by exciting the anthracene residue of the acceptor. The change in the anthracene polarizability by optical excitation is known to be equal to 16.7 Å^3 [41]. Thus, the initial DAC polarizability is $\alpha_0 = 72$ Å^3.

All further calculations depend strongly on the assignment of the initial and final solute dipole moments $m_{g,e}$. For the initial dipole moment we assume $m_g = 0$. A nonzero value of m_g may however be expected based on asymmetry of the DAC and the fact that the acceptor residue is initially in the optically excited state. The final dipole moment can be determined from the separation of the centers of the donor and acceptor moieties assumed to be the centers of electron density localization as well: $m_e = eR = 43.5$ D which is however a rather crude approximation. In view of this uncertainty, the choice of m_e will be dictated by the condition that the vacuum energy gap ΔI is to fall in the range $1.3 \text{ eV} \leqslant \Delta I \leqslant 2.1$ eV estimated above. The calculations are performed according to the procedure outlined in Section 3.2 for the 10 solvents with their properties listed in Table 1 [62,80–82]. For the equilibrium energy gaps ΔG^0, experimental values listed in Table 2 are used [29,75,76]. The effective excitation energy of the DAC I_0 in Eq. (32) is equated to the vacuum energy gap ΔI. The parameter δ in Eq. (32) becomes thus a function of the energy gap ΔI the value of which is therefore found from the iteration procedure as the intercept of the plot of $\Delta G^0 - \Delta G_{dip}$ vs. δ.

For $m_e = 43.5$ D, the plot of $\Delta G^0 - \Delta G_{dip}$ vs. δ from Eq. (32) results in $\Delta\alpha_0 = 263$ Å^3 and $\Delta I = 2.87$ eV. The vacuum energy gap value is thus too high. A slight downward revision of m_e to the value 38 D gives

Table 1
Solvent parameters used in the analysis: diameter σ, Å; polarizability α, Å^3; dipole moment m, D; LJ energy ϵ_{LJ}/k_B, K; liquid expansibility, 10^{-3} K^{-1}; $Td\sigma/dT$, Å; ionization potential I_0, eV

No.	Solvents	σ [a]	α [b]	m [a]	ϵ_{LJ}/k_B [c]	α_p [a]	$Td\sigma/dT$	I_0 [d]
1	methanol	3.77	3.26	1.7	322	1.19	−0.117 [e]	10.83
2	propionitrile	4.73	6.26	3.5	331	1.33		11.84
3	acetone	4.78	6.43	2.69	375	1.45	−0.186 [e]	9.7
4	pyridine	5.15	9.55	2.30	612	1.02	−0.172 [g]	9.28
5	1,2-dichloroethane	5.08	8.33	1.86	588	1.15		11.12
6	dichloromethane	4.62	6.56	1.60	486	1.35	−0.247 [e]	11.13
7	THF	5.10	7.93	1.75	566	1.29		8.9
8	methyl acetate	4.98	6.81	1.61	506	1.42	−0.144 [e]	10.48
9	ethyl acetate	5.40	8.83	1.78	554	1.38	−0.168 [e]	10.39
10	butyl acetate	6.10	12.37	1.84	678	1.17	−0.146 [f]	9.91

[a] Ref. [62]. [b] From Y. Marcus, Ion Solvation (Wiley, New York, 1985). [c] Ref. [80]. [d] Ref. [78]. [e] Refs. [81,82]. [f] Estimated from the WCA theory. [g] From the temperature dependence of the isothermal compressibility according to the data from R.T. Lagemann, D.R. McMillan, Jr. and W.E. Woolf, J. Chem. Phys. 17 (1949) 369.

already a reasonable estimate of the vacuum energy gap of ΔI = 1.97 eV and $\Delta\alpha_0$ = 226 Å^3. These values, therefore, will be accepted for the remainder of the analysis. The plot of $\Delta G^0 - \Delta G_{dip}$ vs. δ is shown in Fig. 6. The points are rather scattered, probably due to experimental errors ($\simeq$ 10 %) and some uncertainties in the solvent parameters used (for instance, the solvent ionization potentials are available with the accuracy of $\simeq$ 5–10%).

In Table 2, we present the calculation results for the solvent variation of the energy gap and SRE components caused by the different types of solute-solvent interactions. Let us first consider the contributions to the energy gap. The dipolar component ΔG_{dip} of ΔG^0 (Eq. (25)) decreases in absolute value, as expected, with decreasing solvent polarity. On the contrary, the dispersion part ΔG_{disp} (Eq. (29)) becomes more negative. The total solvent variation of both components proves to be comparable. Because of this compensating trend, the total free energy gap changes only gradually with solvent polarity. Clearly, the attribution of the solvent energy gap variation solely to dielectric effects, though commonly used, is rather erroneous. The differential solute-solvent dispersion interaction actually contributes heavily to the energy gap solvent variation.

The SRE presented in Table 2 are split into the two components: (i) nonpolar part due to induction and

Table 2
Dispersion ΔG_{disp} and dipolar ΔG_{dip} contributions to the experimental [29] ET free energy gap ΔG^0. Nonpolar λ_{npol} and polar (divided into orientational $\lambda_{dip,p}$ and density $\lambda_{dip,d}$) reorganization energies (all values are in eV). Also shown parameters of differential dispersion interaction $\Delta\gamma$. Solvent numbering is as in Table 1

No.	$\Delta\gamma$	ΔG_{disp}	ΔG_{dip}	ΔG^0	λ_{npol}	$\lambda_{dip,d}$	$\lambda_{dip,p}$
1	21.43	−0.44	−1.81	−0.58	0.02	0.40	1.06
2	10.38	−0.27	−2.56	−0.57	0.17	0.65	1.40
3	12.11	−0.47	−2.03	−0.53	0.06	0.52	1.12
4	8.64	−0.83	−2.07	−0.43	0.13	0.56	0.96
5	8.14	−0.75	−1.57	−0.39	0.05	0.41	0.72
6	10.53	−0.60	−1.45	−0.34	0.02	0.34	0.69
7	10.51	−0.94	−1.35	−0.28	0.04	0.34	0.62
8	10.55	−0.77	−1.30	−0.23	0.02	0.33	0.63
9	8.19	−0.82	−1.13	−0.18	0.02	0.28	0.51
10	6.09	−1.04	−0.94	−0.08	0.09	0.23	0.36

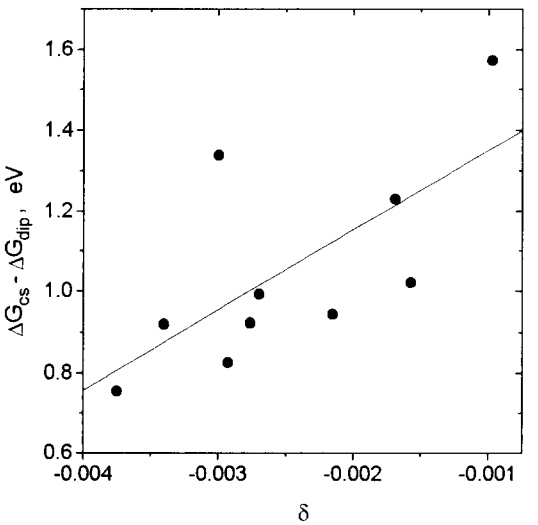

Fig. 6. Plot of the dispersion component of the equilibrium energy gap $\Delta G^{(0)} - \Delta G_{dip}$ vs. the parameter δ determined by Eq. (32) for the 10 solvents (•) from Table 1. ΔG_{dip} values (row 3 in Table 2) are evaluated from Eq. (25) and $\Delta G^{(0)}$ are experimental data (row 4 in Table 2). The solid line is the linear regression.

dispersion forces

$$\lambda_{npol} = \lambda_{disp} + \lambda_{ind}$$

and (ii) the contribution due to reorganization of permanent dipoles. The latter component according to Eq. (6) can be referred to two physically distinct processes: reorientation of the dipoles and their translations. According to Fig. 2 and the discussion in Section 2, the extraction of the orientational term can be performed by turning off the coordinate correlations of the liquid molecules in the total dipolar response function μ_p. This is achieved by assuming the $\rho^* \to 0$ limit in the Padé forms $P_i(y_i, \rho^*, r_0)$ [60]. Inspection of Table 2 shows that the translational (density) component $\lambda_{dip,d}$ so obtained is essentially one-half the orientational reorganization energy $\lambda_{dip,p}$, in agreement with our previous estimates for outer-sphere ET [17,18]. Since both induction and dispersion components of the SRE are caused by molecular translations, we can split the total SRE to translational and orientational parts

$$\lambda_s = \lambda_{or} + \lambda_{tr}, \tag{37}$$

where

$$\lambda_{or} = \lambda_{dip,p} \quad \text{and} \quad \lambda_{tr} = \lambda_{disp} + \lambda_{ind} + \lambda_{dip,d}.$$

The decomposition of the SRE into translational and orientational components [16] is analogous to that suggested by both Bagchi [13] and Ladanyi and Stratt [83] for the nonequilibrium solvation problem. In those studies, polar solvation is classified as coupling into orientational coordinates and nonpolar solvation as coupling into center-of-mass translations. In our present calculations, the nonpolar component remains small relative to λ_{dip} for all solvents excluding weakly polar butyl acetate. Notice that the induction part λ_{ind} is very small in this case due to the large solute size R_0. Therefore, the decoupling assumption (2) should not noticeably affect the calculation procedure.

The splitting of the SRE (37) into the long-range orientational and short range translational solvent responses generates different types of temperature dependencies of the two parts: $\lambda_{or} = \lambda_{dip,p}$ does not contain T explicitly,

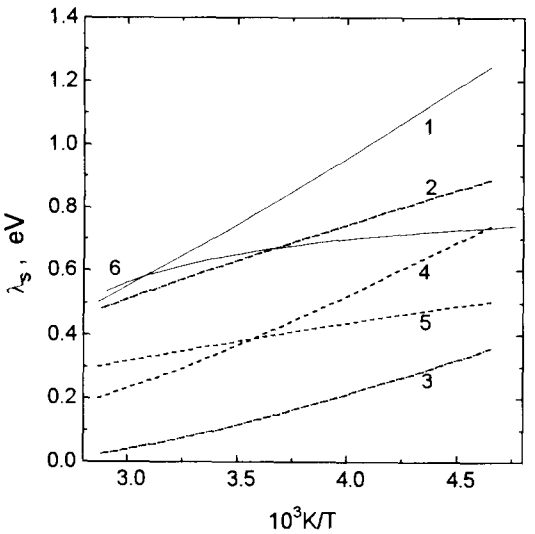

Fig. 7. Calculated temperature variation of the solvent reorganization energy in butyl acetate (1) and its dipolar λ_{dip} (2) and nonpolar λ_{npol} (3) parts. Also shown are the dissection of the total solvent reorganization energy into translational λ_{tr} (4) and orientational λ_{or} (5) constituents and the temperature variation of the continuum SRE of Eq. (15) (6). Solute parameters are: $m_g = 0$, $m_c = 38$ D, $\Delta\alpha = 226$ Å^3, $\Delta\gamma = 6.09$, $\Delta I = 1.97$ eV.

in accordance with the macroscopic fluctuation-dissipation theorem, whereas $\lambda_{tr} \propto 1/T$ [16,18]. As is seen from Eqs. (5) and (8), both reorganization components obtained by a perturbation expansion over the solute-solvent field are proportional to the solvent dipoles density y_0. However, for reorientation of permanent dipoles, this factor is canceled out by the $k = 0$ poles of the longitudinal $m^+(k)$ and transverse $m^-(k)$ structure factors, as is seen from Eq. (11). This leads to the appearance of the usual Pekar factor c_0 in the longitudinal and $c_0\epsilon_s/\epsilon_\infty$ in the transverse parts of the reorganization energy of dipole orientations $\lambda_{dip,p}$. For the density component of solvent reorganization, this cancellation does not occur due to the short-range character of density correlations. As a result, $\lambda_{dip,d} \propto y_0$ and contains therefore the explicit dependence on temperature $\lambda_{dip,d} \propto \beta$.

The main portion of the temperature variation of the SRE is therefore produced by its translational component as is seen in Fig. 7 drawn for butyl acetate. For this solvent, the translational part of the SRE λ_{tr} is smaller than the orientational part λ_{or} at high temperatures, but comes in excess to it at lower temperatures. However, if only permanent dipole modes are included, the $1/T$ temperature variation of the translational reorganization component is compensated in strongly polar solvents by the opposite effect of the orientational part [16,18]. Therefore, the noticeable temperature dependence of the SRE is to be expected when the dipole translations effect is reinforced by the nonpolar component due to dispersions and inductions as for the DAC under consideration (Fig. 7). The relatively small impact of differential dispersive solvation and the compensation between the effects of dipolar translations and reorientations can actually account for the observed small temperature variation of the SRE in mixed-valency complexes [84–86]. Notice in this respect that for symmetrical mixed-valency complexes often claimed to be the best probes of solvent reorganization effects the polarizability variation $\Delta\alpha$ is equal to zero and dispersion forces have no effect on ET energetics. On the other hand, in organic ET systems containing π-orbitals the dispersion forces effect may assume significance because of large solute polarizability variations during ET. This difference may be the reason why the solvent reorganization parameters extracted for symmetrical ET systems cannot be applied directly to ET with a nonzero energy gap. Actually, for the aromatic betaine-30 dye, Walker et al. [87] reported the noticeable temperature decrease of the SRE in weakly polar glycerol triacetate, in qualitative agreement with our present consideration (Fig. 4). The SRE values were extracted from experimental spectroscopic data by employing the hybrid model incorporating intramolecular solute quantum vibrations and the dynamic effect of the solvent polarization and a classical solute vibrational

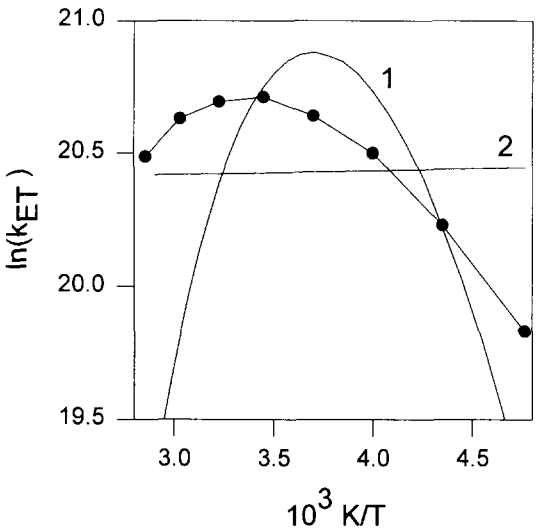

Fig. 8. Temperature variation of the charge separation rate constant in butyl acetate measured experimentally (•) and calculated in the framework of the present (1) and continuum (2) theories. The continuum curve has been shifted downward by 8 units of $\ln(k_{ET})$. The solute parameters are as in Fig. 6.

mode. Although the analysis of Zhu and Rasaiah [88] of the same experimental data yields increasing with T SRE values, the present treatment provides support to the results of Walker et al. [87].

The temperature dependence of the nonpolar component of the reorganization energy has recently been measured by transient hole burning experiments performed on the nonpolar s-tetrasine dye [89]. The Stokes shift amounting to twice the total reorganization energy (including the solvent and the solute parts) was found to be clearly decreasing with temperature. If the intramolecular reorganization energy is temperature independent, the observed decaying temperature variation is to be attributed to the SRE, in agreement with the analogous trend for λ_{npol} of the present paper.

As is seen from Table 2, the translational part of the SRE becomes increasingly important as solvent polarity decreases. For butyl acetate, for instance, the orientational and translational portions of λ_s are almost equal (Table 2). Under these circumstances, the implicit temperature dependence of λ_{tr} may manifest itself in a maximum of the ET rate in the Arrhenius coordinates [16]. This actually happens for ET in butyl acetate, as is shown in Fig. 8, where the experimental temperature variation of the ET rate constant is compared with the calculated one. The ET rate constant is taken in the nonadiabatic form with correction for the intramolecular vibrational modes in the well-known form [90]

$$k_{ET} = \frac{2\pi}{\hbar}\frac{V^2}{\sqrt{4\pi k_B T \lambda_s}}\sum_{n=0}^{\infty}\frac{S^m}{m!}\exp(-S)\exp\left(-\frac{(\Delta G^0 + \lambda_s + n\hbar\omega_i)^2}{4k_B T\lambda_s}\right), \tag{38}$$

where $S = \hbar\omega_i/\lambda_i$, λ_i and ω_i are the reorganization energy and the frequency of a characteristic intramolecular vibration mode, respectively. These parameters are taken to be λ_i = 0.44 eV, ω_i = 1500 cm^{-1} [75]. The electron transfer matrix element V has been taken to be equal to 0.01 eV to match the experimental rate constant. The implicit temperature variation of the SRE and the equilibrium energy gap are caused by the temperature dependent liquid packing density and the HS diameter evaluated as follows

$$\eta(T) = \eta(T_0)\left[1 + \left((3T_0/\sigma)d\sigma/dT - \alpha_p\right)(T - T_0)\right], \qquad \sigma(T) = \sigma(T_0) + (d\sigma/dT)(T - T_0),$$

where T_0 = 298 K, the solvent molecular expansibilities α_p and the solvent-size derivatives $(d\sigma/dT)$ are listed in Table 1.

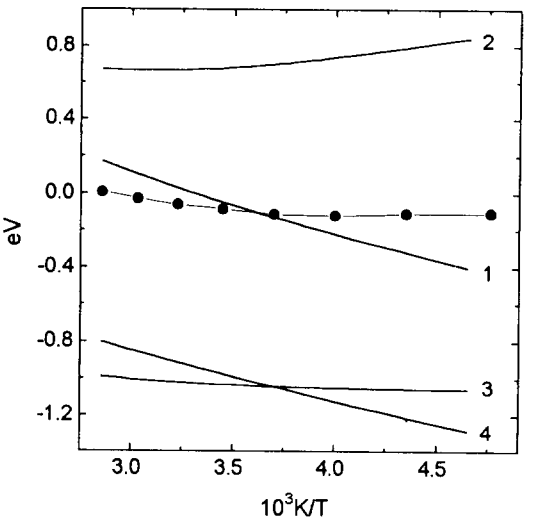

Fig. 9. Temperature dependence of the experimental (•) and calculated (1) equilibrium energy gap ΔG^0 in butyl acetate, its dispersion (3) and dipolar (4) components, and the spectral shift $\Delta G^0 + \lambda_s$ (2). The solute parameters are as in Fig. 6.

The theoretical temperature variation of the ET rate constant is more curved compared to experiment with the maximum at a lower temperature. This can be rooted in a stronger than experimental variation of the calculated equilibrium energy gap (Fig. 9). Since the dispersion component of the energy gap is nearly invariant with temperature (Fig. 9), the mistake should be connected with the dipolar component $\Delta G_{\rm dip}$ being thus the main contributor to the temperature dependence of ΔG^0. This latter observation explains why we previously reproduced successfully the experimental temperature coefficients $d\hbar\omega_{\rm abs}/dT$ of optical absorption lines in nonpolar fluids without invoking the dispersion part of the solvent-induced shift [15].

In the context of the theory–experiment discrepancies, some simplifications peculiar to the present calculation procedure deserve special comment. As concerns the temperature variation of the activation parameters, we assumed here the parameter $\Delta\gamma$ of the dispersive interactions to be temperature and solvent independent. This is certainly a simplification, since the DAC polarizability is strongly dependent on the spectrum of its intramolecular electronic levels varying with both solvent and temperature [91]. However, in view of the disagreement with the experimental temperature variation of the energy gap, the calculation of its dipolar component $\Delta G_{\rm dip}$ seems to be the main source of mistakes. Here, we used the same solute polarizability α_0 in calculating the solute liquid state dipole moments $m'_{g,e}$. Actually, different values of α_0 should be applied for each state. The variation $\Delta\alpha$ found by assuming the London form of solute-solvent dispersion forces is, however, hardly applicable as a real measure of the solute polarizability change and should be treated more properly as an effective parameter of the dispersive solute-solvent attractions. Another assumption made in calculating $\Delta G_{\rm dip}$ is of more fundamental character. The chemical potential of dipole solvation involves the linear response approximation widely used in ET and optical spectroscopy treatments. For the large solute dipole moment $m_{\rm e} \simeq$ 40 D, however, the reduced interaction energy with the adjacent liquid molecules $\beta m'_{\rm e} m'/(r_0\sigma)^3$ amounts for acetone, for instance, to 5.6. At so large interaction energies, higher order terms in the perturbation expansion over the solute dipole moment may become substantial [92]. In fact, nonlinear effects in nonequilibrium solvation have been found even at lower solute-solvent interaction energies [93,94], although related chiefly to the specific forces effect [95]. The extension to nonlinear dipole solvation will be considered elsewhere [96]. That is the reason why the theory presented here is restricted to weakly polar solvents. A unified treatment embracing both strongly and weakly polar solvents is still to be developed.

Another and probably most important source of the too strong temperature variation of the solvation energies

used in the calculations of λ_s and ΔG^0 is the point dipole representation for the solute field $\Delta \boldsymbol{D}(\boldsymbol{r})$. As is seen in Fig. 7, the orientational part $\lambda_{\mathrm{dip,p}}$ is more strongly temperature dependent for the point dipole approximation than in the case of $\lambda^{(c)}_{\mathrm{dip,p}}$ employing the longitudinal solute field (13) and (14). This is the consequence of a large transverse projection in the point dipole field. Application of the nonpoint dipole model would decrease the transverse projection and yield less steep temperature variation of λ_s. Yet this procedure results in a divergent at $\epsilon_s \to \infty$ term in the linear response ansatz. This problem actually invites further investigations. Notice only that our previous study of the ET maxima in the Arrhenius coordinates in terms of longitudinal $\Delta \boldsymbol{D}(\boldsymbol{r})$ of Eqs. (13) and (14) [28] showed less curved dependencies of $\ln(k_{\mathrm{ET}})$ on $1/T$ than that drawn in Fig. 8. In view of the theory shortcomings mentioned and the remaining uncertainty in the solute molecular parameters, we refrain here from a further analysis of ET temperature dependencies focusing more on consideration to the qualitative agreement achieved for ET in butyl acetate.

In spite of the limitations, the present theory proves to be qualitatively superior to traditional continuum treatments. Fig. 8 shows the temperature variation of the rate constant predicted by the continuum Marcus approximation. The rate constant is calculated according to Eq. (38) with the SRE and the energy gap taken, respectively, from Eq. (15) and

$$\Delta G^0 = \Delta I - \left(1 - \frac{1}{\epsilon_s}\right)\frac{e^2}{2R_{\mathrm{a}}} - \left(1 - \frac{1}{\epsilon_s}\right)\frac{e^2}{2R_{\mathrm{d}}} - \frac{e^2}{\epsilon_s R}, \tag{39}$$

The temperature variation of the dielectric constants in Eqs. (15) and (39) is assumed in the linear form

$$\epsilon_{\infty,s}(T) = \epsilon_{\infty,s}(T_0) + \left(d\epsilon_{\infty,s}/dT\right)(T - T_0), \qquad T_0 = 298\ \mathrm{K}.$$

The rate constant resulting from the continuum estimate is noticeably higher then the experimental value and, even more important, there is no maximum. Qualitatively the same result derives from the MSA outer-sphere equation [9,10] similarly based on the dipolar orientational mechanism of ET activation.

Continuum models of solvent effect on ET have the obvious advantage to be simple and can actually handle many aspects of the solvent variation of ET rates [2,3] concerning the solvent dependence of the solvation free energy. The predictive ability of continuum theories becomes but poorer for the enthalpy–entropy splitting of the free energy [18,97] and, in more general terms, for the differential thermodynamic properties as, for instance, activation volume [98]. Moreover, as shown by the above comparison between the molecular and continuum approaches, the occurrence of a maximum in the Arrhenius coordinates presents a qualitative result which cannot be explained in the framework of the continuum concepts. At this point, a molecular description of the solvent including molecular translations becomes necessary, although at the cost of a more complicated theoretical treatment.

5. Summary

The paper reports the development and some applications of a molecular treatment of ET reactions in weakly polar liquids. What we have focused on is the relative importance of different types of solute-solvent interactions in activating ET and the effect of different liquid modes on the temperature variation of ET rates. The equilibrium energy gap and the solvent reorganization energy have been dissected into the contributions from the dispersion and dipolar forces. The latter part was in turn treated as a sum of the contributions from the dipolar orientational and translational motions. Taken together, the parts due to dispersion forces and dipolar translations form the translational contribution to the overall solvent reorganization. In this way, the SRE is grained into the component corresponding to the translational and orientational solvent modes.

Two key results of this study can be summarized as follows. (i) The dispersion and dipolar components of the free energy gap vary in opposite directions with solvent polarity: the dipolar part increases and the dispersion

Table 3
Coefficients of the density expansion of the functions $a(\rho^*)$, $b(\rho^*)$, $c(\rho^*)$ in the integral $I_{0s}^{(3)}$ and $d(\rho^*)$, $e(\rho^*)$ and $f(\rho^*)$ in $I_{0s}^{(2)}$

i	a	b	c	d	e	f
0	1	−9/16	1/32	0	0	0
1	0.6024	0.2547	−0.2562	1.9350	−1.675	0.4390
2	−0.3808	0.8483	−0.2632	−0.9721	2.183	−1.0510
3	−0.0611	−0.1072	−0.0983	0.3982	−0.8311	0.4653

part decreases. The variations of both parts are comparable in magnitude. This compensatory trend is thus to be included in any realistic analysis of the solvent dependence of the equilibrium energy gap. (ii) The difference between the activation mechanisms of ET in strongly polar and weakly polar liquids is rooted in different weights of orientational and translational modes in the total SRE. In strongly polar solvents, the orientational activation mechanism is prevalent. In weakly polar solvents, the components due to dipoles reorientation and molecular translations become approximately equal, with the latter part tending to dominate with decreasing solvent polarity.

The translational component of the SRE provides the main portion of the overall temperature variation of the reorganization energy and is the origin of the maximum in the Arrhenius coordinates obtained here theoretically for butyl acetate and observed previously in experiment.

Acknowledgements

The author gratefully thanks Hans Heitele for hospitality at the Munich Technical University and his critical comments and suggestions on the manuscript. Many thanks also to Roland Schmid for reading the manuscript.

Appendix A. Padé form of the dipolar response

The perturbation expansion up to the fourth order over the dipole–dipole forces (both solute-solvent and solvent-solvent) yields the following form of the solvent response

$$P(y,\rho^*,r_0) = \frac{yI_{0s}^{(2)}}{1 + yI_{0s}^{(3)}/I_{0s}^{(2)}},$$

where $I_{0s}^{(2)}$ and $I_{0s}^{(3)}$, respectively, are two- and three-particle solute-solvent integrals. They have been represented by simple polynoms [60]

$$I_{0s}^{(2)} = \frac{a(\rho^*)}{r_0^3} + \frac{b(\rho^*)}{r_0^4} + \frac{c(\rho^*)}{r_0^6}, \qquad I_{0s}^{(3)} = \frac{1}{r_0^3} + \frac{d(\rho^*)}{r_0^4} + \frac{e(\rho^*)}{r_0^5} + \frac{f(\rho^*)}{r_0^6},$$

where $a(\rho^*)$, $b(\rho^*)$, $c(\rho^*)$, $d(\rho^*)$ and $e(\rho^*)$ are the third order polynoms of ρ^* as, for instance,

$$a(\rho^*) = a_0 + a_1\rho^* + a_2\rho^{*2} + a_3\rho^{*3}.$$

The polynomial coefficients listed in Table 3 have been fitted to the calculated ρ^*- and r_0-dependencies of $I_{0s}^{(2)}$ and $I_{0s}^{(3)}$.

Appendix B. Nomenclature

A_A	electron affinity of the donor site
c_0	$c_0 = 1/\epsilon_\infty - 1/\epsilon_s$ is the Pekar factor
d	$d = 2R_0/\sigma$ is the reduced solute diameter
e	electron charge
E_{ex}	excitation energy of the acceptor moiety
g_K	Kirkwood g factor
$g_{0s}^{(0)}$	solute-solvent hard sphere distribution function
ΔG^0	equilibrium free energy gap
ΔG_{dip}	dipolar component of the equilibrium free energy gap
ΔG_{disp}	dispersion component of the equilibrium free energy gap
$h_{ss}^{(0)}$	spherically symmetrical part of the solvent correlation function
$I_{A,D}$	ionization potential of the acceptor (A) and donor (D) sites in the donor–acceptor complex
I_s	ionization potential of the solvent molecules
I_0	effective ionization potential of the solute, equated to ΔI
ΔI	gas phase energy gap of the solute
m	solvent dipole moment
m_0	solute dipole moment
m'	solvent dipole moment enhanced by the interaction of the molecular polarizability with the field of the surrounding molecules
m_0'	solute dipole moment enhanced by the interaction of the solvent reaction field with the solute polarizability
m_0^∞	solute dipole moment enhanced by the interaction of the solvent high-frequency reaction field with the solute polarizability
m_g	initial state solute dipole moment
m_e	final state solute dipole moment
$m^\pm(k)$	longitudinal ("+") and transverse ("−") structure factors of dipolar fluctuations
$m_\infty^\pm(k)$	longitudinal ("+") and transverse ("−") structure factors of induced dipoles' fluctuations
$m_{ss}(k)$	solvent structure factor
R_d, R_a	radii of the donor (d) and acceptor (a) moieties
R_0	radius of the effective sphere representing the donor–acceptor complex
r_0	$r_0 = R_0/\sigma + 1/2$ is the reduced distance of the closest approach of the solvent molecules to the solute
T	temperature
y_0	$y_0 = (4\pi/9)\beta\rho m^2$ is the permanent dipoles density parameter
y_∞	$y_\infty = (4\pi/3)\rho\alpha$ is the induced dipoles density parameter
y	$y = y_0 + y_\infty$ is the dipolar density parameter

Greek letters

α_0	solute polarizability
α_s	solvent polarizability
α_p	isobaric solvent expansibility
β	$\beta = 1/k_B T$
β_T	isothermal solvent compressibility
γ	characteristic strength of the solute-solvent dispersion coupling
δ	energetic parameter of the solute-solvent dispersion coupling
Δ	$\Delta^2 = 2k_B T\lambda_s$ is the spectral width of the inertial solvent fluctuations
$\epsilon_{LJ}^{(s)}$	solvent Lennard-Jones energy
ϵ_∞	high-frequency solvent dielectric constant
ϵ_s	static solvent dielectric constant
ϵ_{eff}	effective dielectric constant of the solute
η	solvent packing fraction
λ_{dip}	reorganization energy of the solvent permanent dipoles
$\lambda_{dip,p}$	solvent reorganization component due to reorientation of permanent dipoles, the same as λ_{or}
$\lambda_{dip,d}$	solvent reorganization component due to the coordinates variation of permanent dipoles
λ_{disp}	dispersion part of solvent reorganization
λ_i	reorganization energy of the solute intramolecular vibrations
λ_{ind}	reorganization energy of induced solvent dipoles
λ_{npol}	$\lambda_{npol} = \lambda_{disp} + \lambda_{ind}$ is the nonpolar part of the solvent reorganization energy
λ_{tr}	solvent reorganization energy due to the liquid molecular translations
μ_p	chemical potential of the solute dipole solvation
μ_p^∞	high-frequency chemical potential of solvation by induced solvent dipoles
$\mu_{disp}^{(1)}$	first order coefficient of the expansion of the dispersion solvation energy over the strength of the dispersion coupling γ
ρ	solvent number density
ρ^*	$\rho^* = \rho\sigma^3$ is the reduced solvent density
σ	solvent hard sphere diameter
$\sigma_{LJ}^{(0s)}$	solute-solvent Lennard-Jones diameter
$\sigma_{LJ}^{(s)}$	solvent Lennard-Jones diameter
Ψ_p	solvent response function of the solute dipole solvation
Ψ_p^∞	high-frequency solvent response function of the solute dipole solvation
ω_{abs}	absorption electron transfer frequency
ω_{fl}	fluorescence electron transfer frequency
ω_i	characteristic frequency of the solute intramolecular vibrations

References

[1] M.J. Weaver, Chem. Rev. 92 (1992) 463.
[2] J.T. Hupp, Y. Dong, R.L. Blackbourn and H. Lu, J. Phys. Chem. 97 (1993) 3278.
[3] B.S. Brunschwig, S. Ehrenson and N. Sutin, J. Phys. Chem. 90 (1986) 3657.
[4] D.V. Matyushov and R. Schmid, J. Phys. Chem. 98 (1994) 5152.
[5] S. Pekar, Investigations of the Electronic Theory of Crystals, Moscow, 1951.
[6] R.A. Marcus, J. Chem. Phys. 24 (1956) 966; Ann. Rev. Phys. Chem. 15 (1964) 155.
[7] P. Wolynes, J. Chem. Phys. 86 (1987) 5133.
[8] D.Y.C. Chan, D.J. Mitchell and B.W. Ninham, J. Chem. Phys. 70 (1979) 2946.
[9] I. Rips, J. Klafter and J. Jortner, J. Chem. Phys. 88 (1988) 3246; ibid. 88 (1988) 3246.
[10] W.R. Fawcett and L. Blum, Chem. Phys. Lett. 187 (1991) 173.
[11] W.R. Fawcett and M. Opałło, J. Electroanal. Chem. 331 (1992) 815.
[12] L. Perera and M.L. Berkowitz, J. Chem. Phys. 96 (1992) 3092.
[13] B. Bagchi, J. Chem. Phys. 100 (1994) 6658.
[14] S. Ravichandran and B. Bagchi, Int. Rev. Phys. Chem. 14 (1995) 271.
[15] D.V. Matyushov and R. Schmid, Mol. Phys. 84 (1995) 533.
[16] D.V. Matyushov and R. Schmid, J. Chem. Phys. 103 (1995) 2034.
[17] D.V. Matyushov, Mol. Phys. 79 (1993) 795.
[18] D.V. Matyushov, Chem. Phys. 174 (1993) 199.
[19] T. Asahi, M. Ohkohchi, R. Matsusaka, N. Mataga, R.P. Zhang, A. Osuka and K. Maruyama, J. Am. Chem. Soc. 115 (1993) 5665.
[20] G.L. Closs, L.T. Calcaterra, N.J. Green, K.W. Penfield and J.R. Miller, J. Phys. Chem. 90 (1986) 3673.
[21] A.M. Kjaer and J. Ulstrup, J. Am. Chem. Soc. 109 (1987) 1934.
[22] I.R. Gould, D. Noukakis, J.L. Goodman, R.H. Young and S. Farid, J. Am. Chem. Soc. 115 (1993) 3830.
[23] K. Wynne, C. Galli and R.M. Hochstrasser, J. Chem. Phys. 100 (1994) 4797.
[24] J. Cortés, H. Heitele and J. Jortner, J. Phys. Chem. 98 (1994) 2527.
[25] B.M. Britt, J.L. McHale and D.M. Friedrich, J. Phys. Chem. 99 (1995) 6347.
[26] K. Kulinowski, I.R. Gould and A.B. Myers, J. Phys. Chem. 99 (1995) 9017.
[27] J. Morais and M.B. Zimmt, J. Phys. Chem. 99 (1995) 8863.
[28] D.V. Matyushov and R. Schmid, Chem. Phys. Lett. 220 (1994) 359.
[29] H. Heitele, P. Finkch, S. Weeren, P. Pöllinger and M.E. Michel-Beyerle, J. Phys. Chem. 93 (1989) 5173.
[30] E. Vauthey and D. Phillips, Chem. Phys. 147 (1990) 421.
[31] K. Ando, J. Chem. Phys. 101 (1994) 2850.
[32] H.-X. Zhou and A. Szabo, J. Chem. Phys. 103 (1995) 3481.
[33] A. Samanta and S.K. Ghosh, J. Chem. Phys. 102 (1995) 3172.
[34] Y.-P. Liu and M.D. Newton, J. Phys. Chem. 99 (1995) 12382.
[35] S.-H. Chong, S. Miura, G. Basu and F. Hirata, J. Phys. Chem. 99 (1995) 10526.
[36] B.-C. Perng, M.D. Newton, F.O. Reineri and H.L. Friedman, J. Chem. Phys. 104 (1996) 7153; ibid. 7177.
[37] H.J. Kim and J.T. Hynes, J. Chem. Phys. 96 (1992) 5088.
[38] J. Zhu and R.I. Cukier, J. Chem. Phys. 102 (1995) 8398.
[39] P.O. Andersson, T. Gillbro, L. Ferguson and R. Cogdell, Photochem. Photobiol. 54 (1991) 353.
[40] B.L. Burrows and A.T. Amos, Theoret. Chim. Acta 36 (1974) 1.
[41] I. Renge, Chem. Phys. 167 (1992) 173.
[42] W. Liptay, Z. Naturforsch. 20a (1965) 1441.
[43] G. Rauhut, T. Clark and T. Steinke, J. Am. Chem. Soc. 115 (1993) 9174.
[44] E. Leontidis, U.W. Suter, M. Schütz, H.-P. Lüthi, A. Renn and U.P. Wild, J. Am. Chem. Soc. 117 (1995) 7493.
[45] R.F. Loring, J. Phys. Chem. 94 (1990) 513.
[46] N.E. Shemetulskis and R.F. Loring, J. Chem. Phys. 95 (1991) 4756.
[47] J.S. Bader and B.J. Berne, J. Chem. Phys. 104 (1996) 1293.
[48] F.O. Reineri, H. Resat, B.-C. Perng, F. Hirata and H.L. Friedman, J. Chem. Phys. 100 (1994) 1477.
[49] P. Madden and D. Kivelson, Adv. Chem. Phys. 56 (1984) 467.
[50] A. Chandra and B. Bagchi, J. Chem. Phys. 99 (1993) 553.
[51] Y. Zhou, H.L. Friedman and G. Stell, Chem. Phys. 152 (1991) 185.
[52] E. Lippert, Z. Electrochem. 61 (1957) 962.
[53] L. Onsager, J. Chem. Phys. 58 (1936) 1486.
[54] M.S. Wertheim, J. Chem. Phys. 55 (1971) 4291.
[55] D. Isbister and R.J. Bearman, Mol. Phys. 28 (1974) 1297.

[56] B.C. Freasier and D. Isbister, Mol. Phys. 38 (1979) 81.
[57] G. van der Zwan and J.T. Hynes, J. Phys. Chem. 89 (1985) 4181.
[58] T. Fonseca, B.M. Ladanyi and J.T. Hynes, J. Phys. Chem. 96 (1992) 4085.
[59] M. Maroncelli, J. Chem. Phys. 94 (1991) 2084.
[60] D.V. Matyushov and R. Schmid, J. Chem. Phys. 105 (1996), in press.
[61] M.S. Wertheim, Mol. Phys. 37 (1979) 83.
[62] R. Schmid and D.V. Matyushov, J. Phys. Chem. 99 (1995) 2393.
[63] V. Luzhkov and A. Warshel, J. Am. Chem. Soc. 113 (1991) 4491.
[64] D.J. Giesen, J.W. Storer, C.J. Cramer and D.G. Truhlar, J. Am. Chem. Soc. 117 (1995) 1057.
[65] J. Zeng, N.S. Hush and J.R. Reimers, J. Chem. Phys. 99 (1993) 1508.
[66] H. Reiss, H.L. Frisch and J.L. Lebowitz, J. Chem. Phys. 31 (1959) 369; H. Reiss, Advan. Chem. Phys. 9 (1965) 1.
[67] R.D. Cannon, Chem. Phys. Lett. 49 (1977) 299.
[68] E.D. German, Chem. Phys. Lett. 64 (1979) 295.
[69] T. Boublik, Mol. Phys. 27 (1974) 1415.
[70] T. Boublik, J. Chem. Phys. 53 (1970) 471.
[71] G.A. Mansoori, N.F. Carnahan, K.E. Starling and T.W. Leland, Jr., J. Chem. Phys. 54 (1971) 1523.
[72] J.A. Barker and D. Henderson, Rev. Mod. Phys. 48 (1976) 687.
[73] K.J. Miller, J. Am. Chem. Soc. 112 (1990) 8533.
[74] P. Finckh, H. Heitele, M. Volk and M.E. Michel-Beyerle, J. Phys. Chem. 92 (1988) 6584.
[75] H. Heitele, F. Pöllinger, S. Weeren and M.E. Michel-Beyerle, Chem. Phys. 143 (1990) 325.
[76] H. Heitele, F. Pöllinger, S. Weeren and M.E. Michel-Beyerle, Chem. Phys. Lett. 168 (1990) 598.
[77] S. Zilberg, Y. Haas and S. Shaik, J. Phys. Chem. 99 (1995) 16558.
[78] Handbook of Spectroscopy, ed. J.W. Robinson, vol. 1 (CRC Press, Cleveland, 1974).
[79] P. Kebarle and S. Chowdhury, Chem. Rev. 87 (1987) 513.
[80] D.V. Matyushov and R. Schmid, J. Chem. Phys. 104 (1996) 8627.
[81] D. Ben-Amotz and D.R. Herschbach, J. Phys. Chem. 94 (1990) 1038.
[82] D. Ben-Amotz and K.G. Willis, J. Phys. Chem. 97 (1993) 7736.
[83] B.M. Ladanyi and R.M. Stratt, J. Phys. Chem. 100 (1996) 1266.
[84] J.T. Hupp, G.A. Neyhard and T.J. Meyer, J. Phys. Chem. 96 (1992) 10820.
[85] Y. Dong and J.T. Hupp, Inorg. Chem. 31 (1992) 3322.
[86] Y. Dong and J.T. Hupp, J. Am. Chem. Soc. 115 (1993) 6428.
[87] G.C. Walker, E. Åkesson, A.E. Johnson, N.E. Levinger and P.F. Barbara, J. Phys. Chem. 96 (1992) 3728.
[88] J. Zhu and J.C. Rasaiah, J. Chem. Phys. 101 (1994) 9966.
[89] J. Ma, D.V. Bout and M. Berg, J. Chem. Phys. 103 (1995) 9145.
[90] N.R. Kestner, Y. Logan and J. Jortner, J. Phys. Chem. 78 (1974) 2148.
[91] D. Lu, G. Chen, J.W. Perry and W.A. Goddard, III, J. Am. Chem. Soc. 116 (1994) 10679.
[92] L. Verlet and J.-J. Weis, Mol. Phys. 28 (1974) 665.
[93] E.A. Carter and J.T. Hynes, J. Chem. Phys. 94 (1991) 5961.
[94] T. Fonseca and B.M. Ladanyi, J. Phys. Chem. 95 (1991) 2116.
[95] P.V. Kumar and M. Maroncelli, J. Chem. Phys. 103 (1995) 3038.
[96] D.V. Matyushov and B.M. Ladanyi, in preparation.
[97] B. Roux, H.-A. Yu and M. Karplus, J. Phys. Chem. 94 (1990) 4683.
[98] T.W. Swaddle, Inorg. Chem. 29 (1990) 5017.